Probabilistic Smoothing Based Generation of a Reliable Lane Geometry Map With Uncertainty of a Lane Detector

SEOKWON KIM[1], (Student Member, IEEE), **MINCHUL LEE**[2], (Member, IEEE),
MYOUNGHO SUNWOO[2], (Life Member, IEEE), AND **KICHUN JO**[3], (Member, IEEE)

[1]Global ADAS BU, Mando Corporation, Seongnam 13486, South Korea
[2]Department of Automotive Engineering, Hanyang University, Seoul 133-791, South Korea
[3]Department of Smart Vehicle Engineering, Konkuk University, Seoul 05029, South Korea

Corresponding author: Kichun Jo (kichun.jo@gmail.com)

ABSTRACT Since lane geometry information can be used for controlling the pose of an intelligent vehicle, a lane geometry map that contains the lane geometry information should have reliable accuracy. For generating the reliable lane geometry map, lane curve which is detected from a lane detector is an useful information because the lane geometry information can be obtained directly. However, since the detected lane curve contains an uncertainty caused by the noise of the lane detector, the accuracy of the lane geometry map can be degraded. In previous studies, a near point on each detected lane is sampled at each time stamp and accumulated for reducing the noise effects of the lane detector. However, these sampled points also contain the sensing noise of the lane detector and the density of accumulated points depends on the distance interval of data acquisition. In this article, we proposed the probabilistic lane smoothing-based generation method for the reliable lane geometry map. In the probabilistic lane smoothing, the lane geometry map is modeled as the nodes with the uncertainty of its position obtained from the sensor error model. Each node of the lane geometry map is smoothed based on the Bayesian filtering scheme. The evaluation results show that the lane geometry map can be generated by reducing the noise of the detected lane curve. Additionally, the generated lane geometry map is more reliable than the sampling point-based generated map in terms of the accuracy of the distance and heading angle.
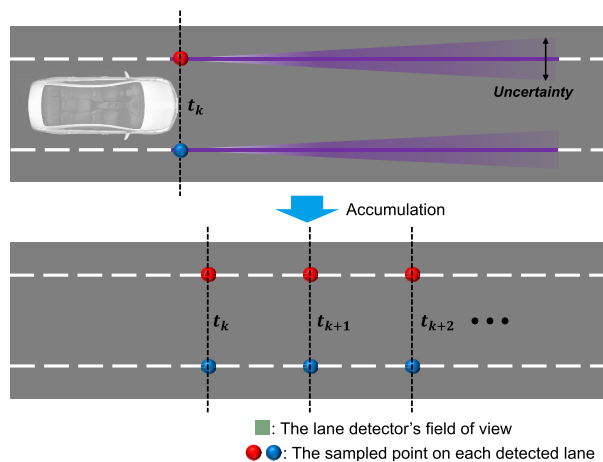
INDEX TERMS Lane geometry map, sensor error model, probabilistic smoothing, Bayesian filtering, lane model.

I. INTRODUCTION

The proportion of traffic accidents caused by human errors such as drowsiness driving, using smart-phones, and inadequate judgment accounts for 94% of the total. According to the National Highway Traffic Safety Administration (NHTSA) in North America, it is expected that 80% of the accidents caused by human errors can be reduced

The associate editor coordinating the review of this manuscript and approving it for publication was Gang Mei.

that the vehicles become intelligent [1]. In this perspective, the intelligent vehicles have been developed from Advanced Driving Assistance Systems (ADAS) to an autonomous driving [2], [3]. For the intelligent vehicles, the surrounding road conditions such as road boundary and lane geometry should be perceived. Among these kinds of the road conditions, the lane geometry information can be used in various applications of the intelligent vehicles such as lane keeping systems [4], [5], vehicle path or motion planning [6]–[9] and in-lane positioning of the ego-vehicle [10]–[15].

S. Kim *et al.*: Probabilistic Smoothing Based Generation of a Reliable Lane Geometry Map With Uncertainty of a Lane Detector

IEEE*Access*

FIGURE 1. Concepts of the sampling-based approaches for generating the lane geometry map.

FIGURE 2. Limitations of the sampling-based lane geometry map generation.

In order to perceive the surrounding lane geometry information, the perception sensors such as camera and Light Detection And Range (LiDAR) are widely used [16]–[20]. However, the lane geometry information from the perception sensors has the sensor noise and detection failure problems. In order to avoid these problems, lane geometry recognition methods with the precise map which contains road boundary, road geometry, and lane geometry have been studied [21]–[25]. Since the lane geometry information is extracted from the precise map in the the precise map-based lane geometry recognition methods, the reliability of the lane geometry information in the precise map should be guaranteed as the accuracy [25].

The lane geometry map should have a centimeter-level position accuracy. Since the width of the lane marker is usually about 20 cm, the position accuracy of the lane geometry map should be satisfied under 20 cm for deciding the ego lane correctly. In addition, the heading angle of the lane geometry can be used to determine the reference heading angle for controlling vehicle pose [4], [5], [26]. Therefore, in order to prevent the instability of the controlled vehicle pose, the heading angle error should be minimized.

For generating the reliable lane geometry map, the detected lane curve from a lane detector is useful information, because the detected lane curve only contains the lane geometry information, not other road conditions. The detected lane curve has a higher uncertainty with a farther distance from the lane detector due to the resolution of the sensors and vehicle motion. Therefore, in the previous studies, a near point on each detected lane is sampled at each time stamp and accumulated for reducing the noise effects of the lane detector as shown in Fig. 1. [12], [27], [28]. However, the sampled points also contain the sensing noise caused by the resolution of the lane detector, painting conditions of the lane markers and potholes. In addition, the density of the accumulated points depends on the distance interval of data acquisition. For example, since the distance interval of data acquisition increases when the probe vehicle drives faster, the distance
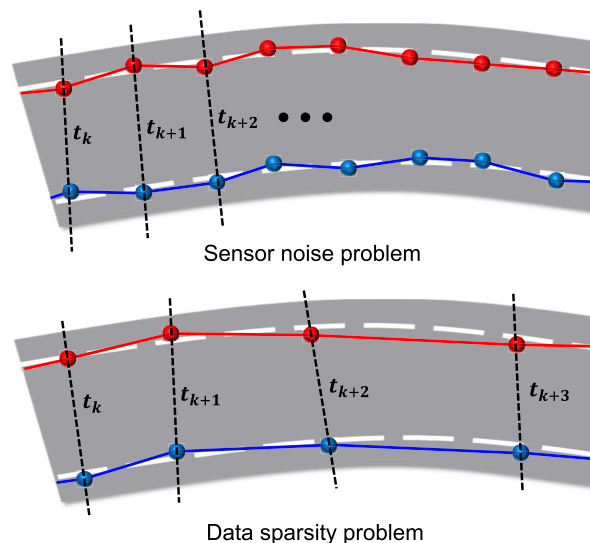
between each point which is sampled at each time stamp also increases. The noise and data sparsity of the sampled points cause the inaccuracy of the generated lane geometry map as shown in Fig. 2.

In order to overcome the limitations of the previous methods, this article proposes the generation method of the reliable lane geometry map based on probabilistic smoothing for considering the uncertainty of the lane detector.

- The lane geometry map is modeled as nodes with the uncertainty of each position.
- The uncertainty of each lane curve is obtained from the sensor error model.
- The position of each node is updated with the lane curves, which are accumulated by the probe vehicle with a lane detector, based on the Bayesian filtering scheme.

This article is organized as follows. Chapter II describes the previous studies, and chapter III represents the system architecture of the proposed system. Chapter IV describes the vehicle trajectory estimation method for solving the multipath error and the signal outage problems of the GPS information. In Chapter V, the probabilistic lane smoothing method is proposed to reduce the noise of the detected lane. Chapter VI describes the lane geometry modeling method for modeling the lane geometry map as a B-spline curve. The lane geometry map generated from the proposed method was verified by comparing the precise digital map which contains the road surface marker in Chapter VII. At the end of this article, the conclusion and the future works are given.

II. RELATED WORKS

For generating the reliable lane geometry map, many approaches have been studied to extract the lane geometry from various types of acquired data. For example, the aerial images from a satellite or an aerial vehicle can be used to
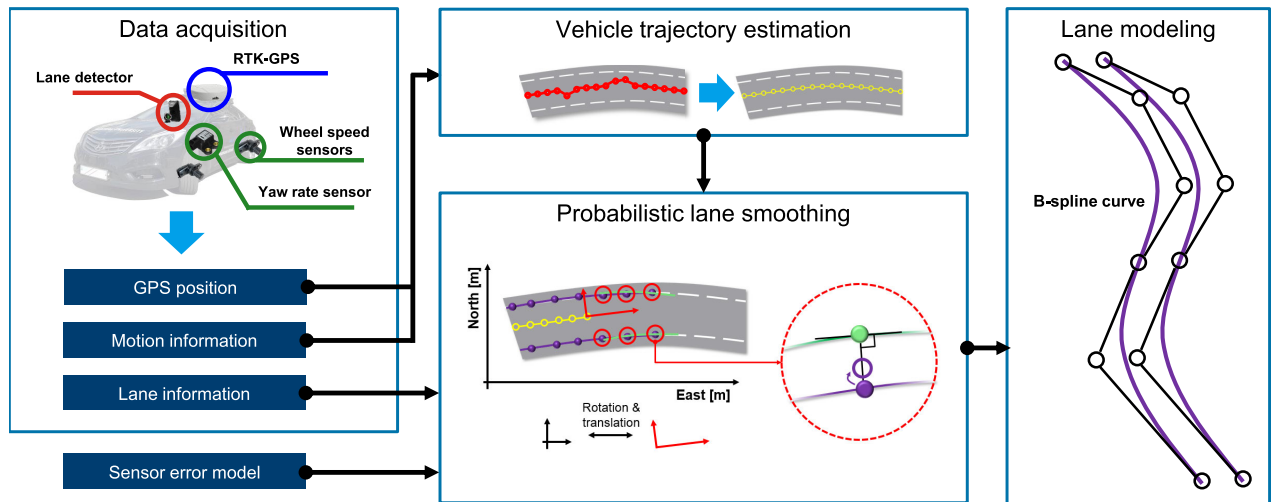
FIGURE 3. Overall system architecture for the proposed lane map generation method.

extract the lane geometry through manual or image processing [29]–[32]. The aerial image can cover large region just in a single image. However, resolution of the aerial image is insufficient to guarantee the accuracy of the lane geometry map [25]. Additionally, there are so many of blocked area occluded by tunnels or road structures such as bridges and underpasses.

Unlike the aerial image-based approaches, the probe vehicle-based approaches acquired the information for the surrounding road condition using the probe vehicle equipped with the perception sensors such as camera or LiDAR [25], [33]–[40]. In these approaches, the surrounding road information is acquired by driving the probe vehicle in forms of the image or point cloud. Since the acquired information does not contain the lane geometry information, the lane information should be extracted from the acquired information. However, in the lane extraction process, the outlier problems are caused by non-lane features such as arrow marks, crosswalks, and surrounding vehicles. These outliers can occur the inaccuracy of extracted lane geometry.

The detected lane curve from the lane detector is more useful information than the accumulated point clouds and the image, because the detected lane curve only contains the lane geometry information, not other road conditions. However, the detected lane curve has an uncertainty caused by the resolution of the sensors and vehicle motion. In the previous studies, a near point of detected lane at each time stamp is sampled and accumulated for reducing the noise effect of the lane detector [12], [27], [28]. In these studies, the density of the accumulated points can be affected by the distance interval of data acquisition. When the probe vehicle moves faster, the distance interval of accumulated points is increased. In addition, the near points also contains the noise caused by the sensor resolution and the condition of the lane marker. Data sparsity and noise problem can cause the inaccuracy of the generated lane geometry map.

In order to overcome the limitations of the previous studies, the probabilistic smoothing based map generation method is proposed in this article. In the proposed method, the lane geometry map is modeled by nodes which are generated from detected lane information. Each node has the uncertainty of its position, and the position of each node is updated probabilistically with accumulated lane information which located by near the node. Unlike the previous studies which use just a sampled point from each time stamp, the proposed method can reduce the inaccuracy of the lane geometry map, because some lane information are used for determining the position of each node and the sensor error model is applied for considering the uncertainty of the lane detector.

III. SYSTEM ARCHITECTURE

The overall structure of the proposed method for generating the lane geometry map consists of four steps; data acquisition, vehicle trajectory estimation, probabilistic lane smoothing, and lane modeling as shown in Fig. 3.

In the first step, time synchronized raw data for the lane geometry map generation such as GPS position, vehicle motion information, and detected lane information are acquired by a probe vehicle equipped with Real-Time Kinematic (RTK) GPS, wheel speed sensors, yaw rate sensor, and lane detector.

The second step is a vehicle trajectory estimation. The RTK-GPS has a centimeter-level accuracy under a reliable GPS signal condition. The reliability of the RTK-GPS can be worsened by multipath error and signal outage problem. Since it is possible to detect the RTK-GPS malfunctions by using the vehicle motion constraints, the vulnerability of the RTK-GPS can be solved by data fusion with the vehicle motion information [41], [42]. In order to improve the reliability of the RTK-GPS information, the Rauch-Tung-Striebel (RTS) smoother is used to estimate the probe vehicle's trajectory as proposed in [43].

S. Kim et al.: Probabilistic Smoothing Based Generation of a Reliable Lane Geometry Map With Uncertainty of a Lane Detector

IEEE Access

The third step is probabilistic lane smoothing. Since the detected lane information contains the sensing noise, the detected lane information should be smoothed for generating the lane geometry map. For smoothing the detected lane information, the lane geometry map is modeled as the nodes with uncertainty of its position. The nodes could be updated using the Bayesian filtering scheme with the detected lane information at time step t_k. In order to update the nodes probabilistically, the reliability of the detected lane information should be modeled using the sensor error model. The error model of the lane detector can be obtained based on the cumulative distribution function of the Gaussian probabilistic distribution.

The final step is a lane modeling. The representation as the sequential nodes is not suitable for the intelligent vehicle systems because an enormous data storage is needed to save the overall lane geometry map data; additionally, the computation burdens are increased to process the lane geometry map data [35]. The data storage can be reduced using the mathematical curve model because the sequential nodes can be compressed mathematical curve equation. In this perspective, the lane geometry map is modeled as a B-spline curve in the lane modeling step as proposed in [43].

IV. VEHICLE TRAJECTORY ESTIMATION

When the probe vehicle acquires the data for generating the lane geometry map, the global position of the probe vehicle is a dominant factor for recognizing where the probe vehicle is. In order to acquire the global position of the probe vehicle, the RTK-GPS which has a centimeter-level accuracy is used in this article.

A. RAUCH-TUNG-STRIEBEL SMOOTHER

Since it is possible to detect the RTK-GPS malfunctions by using the vehicle motion constraints, the reliability of the RTK-GPS information can be improved by data fusion with the vehicle motion information. In order to improve the reliability of the measured RTK-GPS information, the RTS smoother which is one of the fixed-interval optimal smoother is used in this article as proposed in [43]. Since the lane geometry map is generated in offline after completing the data acquisition, the all acquired measurements in a fixed time interval can be used for the fixed-interval optimal smoothing.

1) SYSTEM AND MEASUREMENT MODEL

The probe vehicle's position at the next time step can be predicted using the vehicle motion information such as speed V and yaw rate $\dot{\psi}$. The predicted probe vehicle's position is used as the vehicle motion constraints for detecting the RTK-GPS malfunction as shown in Fig. 4. The equation for predicting the probe vehicle's position is described in (1), The system state x_k which contains vehicle's global position X and Y, and the vehicle's heading angle ψ at time step t_k can be obtained by using the previous system state x_{k-1} and the vehicle motion information; vehicle speed V_{k-1} and yaw rate ψ_{k-1}. Noise ω_k of the system model is the Gaussian
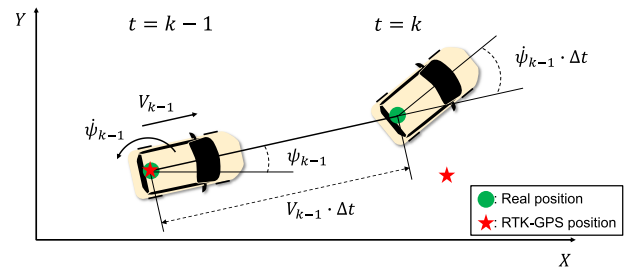

FIGURE 4. Detection of the RTK-GPS malfunction using the predicted probe vehicle's motion.

zero-mean white noise with covariance Q_k.

$$x_k = f(x_{k-1}, u_{k-1}, \omega_{k-1}), \quad \omega_k \sim (0, Q_k)$$
$$\begin{bmatrix} \psi_k \\ X_k \\ Y_k \end{bmatrix} = \begin{bmatrix} \psi_{k-1} + \dot{\psi}_{k-1}\Delta t \\ X_{k-1} + V_{k-1}\Delta t \cos(\psi_{k-1}) \\ Y_{k-1} + V_{k-1}\Delta t \sin(\psi_{k-1}) \end{bmatrix} + \omega_{k-1} \quad (1)$$

The measurements from the RTK-GPS include the global position X_{GPS} and Y_{GPS}, and the heading angle ψ_{GPS}. Since the measurements have a linear relationship to the system state, the observation matrix H_k of the measurement model can be defined as an identity matrix as described in (2). Noise v_k of the measurement model is the Gaussian zero-mean white noise with covariance R_k.

$$y_k = H_k x_k + v_k, \quad v_k \sim (0, R_k)$$
$$\begin{bmatrix} \psi_{GPS_k} \\ X_{GPS_k} \\ Y_{GPS_k} \end{bmatrix} = \begin{bmatrix} 1 & 0 & 0 \\ 0 & 1 & 0 \\ 0 & 0 & 1 \end{bmatrix} \begin{bmatrix} \psi_k \\ X_k \\ Y_k \end{bmatrix} + v_k \quad (2)$$

Since the system model for predicting the probe vehicle's position is a non-linear equation, the extended-Kalman filter is used for the state estimation. The discrete-time extended RTS smoother consists of two steps; forward filter and backward filter [44].

2) FORWARD FILTERING

The initial state and covariance of the forward filter are assumed as the stochastic expected value of the initial state and covariance as described in (3). The subscript f means the forward filter.

$$\hat{x}_{f0}^+ = E(x_0)$$
$$P_{f0}^+ = E\left[(x_0 - \hat{x}_{f0}^+)(x_0 - \hat{x}_{f0}^+)^T\right] \quad (3)$$

In the forward filtering step of the RTS smoother, the extended-Kalman filter is used to estimate the state at time step t_k in the fixed-time interval $k = 1, \ldots, N$ where N is the final time index because the system model for predicting the probe vehicle's position is a non-linear equation. In the time update of the extended-Kalman filter, the state and covariance can be predicted by considering the vehicle motion information as described in (4).

$$\hat{x}_{f,k}^- = f_{k-1}(\hat{x}_{f,k-1}^+, u_{k-1}, 0)$$

$$P_{f,k}^- = F_{k-1}P_{f,k-1}^+ F_{k-1}^T + L_{k-1}Q_{k-1}L_{k-1}^T \qquad (4)$$

Since the system model is a non-linear equation as described in (1), the Jacobian equations of the system model should be obtained based on (5).

$$F_{k-1} = \left. \frac{\partial f_{k-1}}{\partial x} \right|_{\hat{x}_{f,k-1}^+}$$

$$L_{k-1} = \left. \frac{\partial f_{k-1}}{\partial \omega} \right|_{\hat{x}_{f,k-1}^+} \qquad (5)$$

In the measurement update step of the extended-Kalman filter, the state and covariance can be updated by considering the RTK-GPS measurements as described in (6).

$$K_{f,k} = P_{f,k}^- H_k^T (H_k P_{f,k}^- H_k^T + M_k R_k M_k^T)^{-1}$$
$$\hat{x}_{f,k}^+ = \hat{x}_{f,k}^- + K_{f,k}\left[y_k - h_k(\hat{x}_{f,k}^-, 0) \right]$$
$$P_{f,k}^+ = (I - K_{f,k}H_k)P_{f,k}^- \qquad (6)$$

In contrast to the time update step, the measurement model is a linear equation as described in (2). Therefore, the Jacobian equation of the measurement model is not needed for the measurement update step.

3) BACKWARD FILTERING

In the forward filtering of the RTS smoother, the state x_k is estimated just by updating with the measurements before time step t_k. If the measurements after the time step t_k are considered when the state x_k is estimated, the accuracy and reliability of the estimated state can be improved. In the backward filtering of the RTS smoother, the state x_k is estimated in the reverse fixed-time interval $k = N, \ldots, 1$ as described in (7). The subscript b means the backward filter.

$$K_{b,k} = P_{f,k}^+ F_k^T (P_{f,k+1}^-)^{-1}$$
$$P_{b,k} = P_{f,k}^+ - K_{b,k}(P_{f,k+1}^- - P_{b,k+1})K_{b,k}^T$$
$$\hat{x}_{b,k} = \hat{x}_{f,k}^+ + K_{b,k}(\hat{x}_{b,k+1} - \hat{x}_{f,k+1}^-) \qquad (7)$$

The initial state $\hat{x}_{b,N}$ and covariance $P_{b,N}$ for the backward filter can be obtained from the end of the forward filter as described in (8).

$$\hat{x}_{b,N} = \hat{x}_{f,N}^+$$
$$P_{b,N} = P_{f,N}^+ \qquad (8)$$

V. PROBABILISTIC LANE SMOOTHING

A. SENSOR ERROR MODEL

Since the detected lane information contains the discontinuity problems caused by the sensor noise. Therefore, the multiple detected lane information should be smoothed to reduce the discontinuity problems for generating the lane geometry map. In order to smooth the detected lane information probabilistically, the reliability of the detected lane information should be modeled using the sensor error model. The detected lane information has a lower reliability with a farther distance
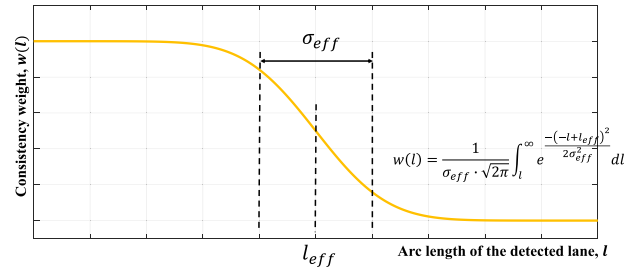
FIGURE 5. Sensor error model with the consistency weight regarding the arc length of the detected lane.
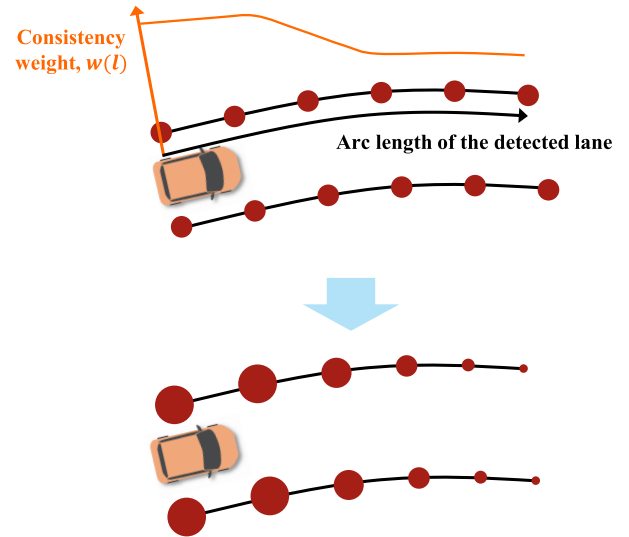
FIGURE 6. Sampled points at regular intervals with the consistency weight.

from the perception sensor. The reliability of the detected lane information can be modeled as the consistency weight $w(l)$ as shown in Fig. 5. [45].

The consistency weight $w(l)$ is modeled based on the modified cumulative distribution function of a Gaussian probabilistic distribution with $N(l_{eff}, \sigma_{eff}^2)$ as described in (9). l_{eff} means the effective distance which represents the valid range of the detected lane information and σ_{eff} means the standard deviation of the effective distance uncertainty.

$$w(l) = \frac{1}{\sigma_{eff} \cdot \sqrt{2\pi}} \int_l^\infty e^{\frac{-(-l+l_{eff})^2}{2\sigma_{eff}^2}} dl \qquad (9)$$

B. BAYESIAN FITLERING-BASED PROBABILISTIC LANE SMOOTHING

1) INITIALIZATION

In order to initialize for generating the lane geometry map in the proposed method, the detected lane information is accumulated. First, the detected lane information is sampled as points with regular intervals. Each sampled point has the consistency weight which represents the reliability of the position information obtained from the sensor error model as shown in Fig. 6.

S. Kim *et al.*: Probabilistic Smoothing Based Generation of a Reliable Lane Geometry Map With Uncertainty of a Lane Detector

IEEE *Access*
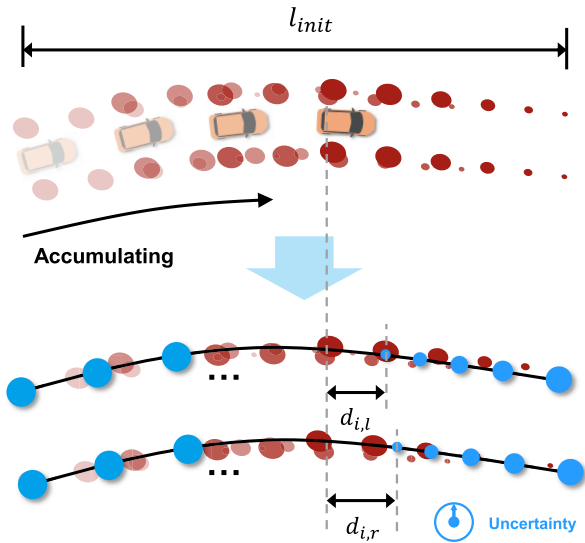
FIGURE 7. Initialization for the lane geometry map by accumulating the weighted sampled point and applying the weighted least square method.

Weighted sampled points are accumulated until the accumulated length is longer than the minimal length l_{init} to initialize the lane geometry map. From these accumulated points, the initial lane geometry map can be approximated based on the weighted least square method using the weight of each accumulated point as shown in Fig. 7.

The nodes of the initialized lane geometry map have the covariance which represents the reliability of their position information. The covariance of each node can be obtained from the sensor error model depending on each node's position as described in (10). Subscript i and j mean the node and the location index of each lane.

$$\begin{cases} P_{i,j} = x(d_{i,j})^{-1} \cdot I & if \ d_{i,j} \in [0, \infty) \\ P_{i,j} = P_{init} \cdot I & if \ d_{i,j} \in (-\infty, 0) \end{cases} \quad (10)$$

2) COORDINATE UPDATE

In order to update the lane geometry map, the detected lane information is used. However, since the lane geometry map is on the global coordinates and the detected lane information is on the ego vehicle's coordinates, the coordinates conversion must be preceded. If the coordinates of the detected lane information are converted from the coordinates of the ego vehicle to the global coordinates, the detected lane information is represented as a non-linear equation. Comparing with the case when the representation of the detected lane information is a linear equation, it is hard to find the nearest measurement point from each node for updating each node of the lane geometry map. Therefore, in order to update the lane geometry map with the detected lane information at time step t_k, the coordinates of the lane geometry map should be converted from the global coordinates to the ego vehicle coordinates. The conversion relationship consists of two parts; translation and rotation as shown in Fig. 8.
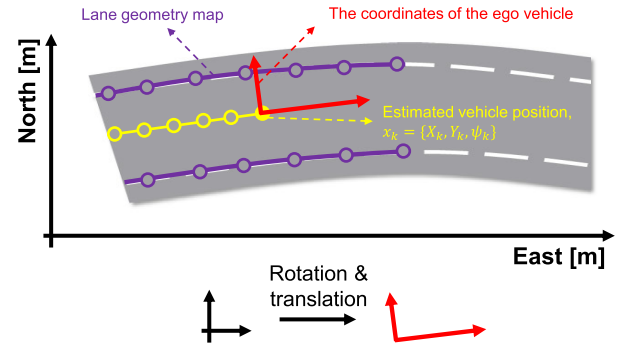
FIGURE 8. Relationship for coordinates conversion from the global coordinates to the ego vehicle coordinates.

The rotation matrix $R_{k,ego}$ and translation matrix $T_{k,ego}$ can be obtained by using the estimated vehicle position x_k which contains the vehicle's heading angle ψ_k, and the vehicle's global position X_k and Y_k. The rotation matrix $R_{k,ego}$ consists of the trigonometrical function with the vehicle's heading angle ψ_k from the estimated vehicle position x_k. The translation matrix $T_{k,ego}$ consists of the relative position from the vehicle's global position X_k and Y_k as described in (11).

$$R_{k,ego} = \begin{bmatrix} \cos(-\psi_k) & -\sin(-\psi_k) \\ \sin(-\psi_k) & \cos(-\psi_k) \end{bmatrix}$$
$$T_{k,ego} = \begin{bmatrix} -X_k \\ -Y_k \end{bmatrix} \quad (11)$$

The converted position of each node of the lane geometry map can be obtained by applying the translation matrix $T_{k,ego}$ and rotation matrix $R_{k,ego}$ as described in (12).

$$\begin{bmatrix} X_{i,j,ego} \\ Y_{i,j,ego} \end{bmatrix} = R_{k,ego} \left(\begin{bmatrix} X_{i,j,world} \\ Y_{i,j,world} \end{bmatrix} + T_{k,ego} \right) \quad (12)$$

3) MEASUREMENT UPDATE

After the coordinates of the lane geometry map was converted from the global coordinates to the ego vehicle's coordinates, the position of each node of the lane geometry map can be updated using the detected lane information at time step t_k. In order to update the position of each node, the measurement point should be selected from the detected lane information. The nearest measurement point $Z_{i,j}$ within a certain boundary from each node is used as the measurement point for updating the position of each node as shown in Fig. 9.

The nearest measurement point $Z_{i,j}$ from each node is represented by its position on the ego vehicle coordinates as described in (13).

$$Z_{i,j} = \begin{bmatrix} X_{meas,ego} \\ Y_{meas,ego} \end{bmatrix} \quad (13)$$

The covariance of the measurement point which means the reliability of the position can be obtained based on the sensor error model depending on the arc length $l_{i,j,meas}$ of the detected lane information to the measurement point as
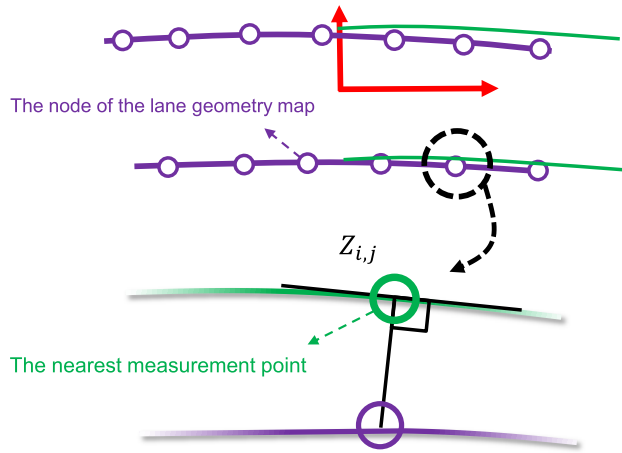
IEEE *Access*

S. Kim *et al.*: Probabilistic Smoothing Based Generation of a Reliable Lane Geometry Map With Uncertainty of a Lane Detector

FIGURE 9. Nearest measurement point for updating the position of each node.

described in (14).

$$P_{i,j,meas} = \begin{bmatrix} w(l_{i,j,meas})^{-1} & 0 \\ 0 & w(l_{i,j,meas})^{-1} \end{bmatrix} \quad (14)$$

In order to update the position and covariance of each node of the lane geometry map probabilistically, the Bayesian filtering scheme is used. A Kalman gain $K_{i,j}$ is calculated based on the measurement point's covariance $P_{i,j,meas}$ and the priori covariance of each node $P_{i,j}^-$. The posteriori position of each node $[X_{i,j,ego}^+, Y_{i,j,ego}^+]^T$ and posteriori covariance of each node $P_{i,j}^+$ can be calculated as described in (15).

$$K_{i,j} = P_{i,j}^-(P_{i,j}^- + P_{i,j,meas})^{-1}$$
$$P_{i,j}^+ = (I - K_{i,j})P_{i,j}^-$$
$$\begin{bmatrix} X_{i,j,ego}^+ \\ Y_{i,j,ego}^+ \end{bmatrix} = \begin{bmatrix} X_{i,j,ego}^- \\ Y_{i,j,ego}^- \end{bmatrix}$$
$$+ K_{i,j}\left(Z_{i,j} - \begin{bmatrix} X_{i,j,ego}^- \\ Y_{i,j,ego}^- \end{bmatrix}\right) \quad (15)$$

The new node of the lane geometry map is generated using the end point of the detected lane information. If the distance d between the end point of the detected lane information and the end node of the lane geometry map is larger than the predefined threshold d_{new}, the new node of the lane geometry map is generated on the position of the end point of the detected lane information. The covariance of the new node is initialized by using the covariance of the end measurement point which is obtained based on the sensor error model as described in (16).

$$\begin{bmatrix} X_{new,j,ego} \\ Y_{new,j,ego} \end{bmatrix} = Z_{end,j}, \quad P_{new,j} = P_{end,j,meas} \quad (16)$$

When the intelligent vehicle uses the lane geometry map, the lane geometry map around the vehicle is found based on the global position of the vehicle. Therefore, the node of the lane geometry map should be on the global coordinates.

Similar to the coordinate update step, the rotation matrix $R_{k,world}$ and translation matrix $T_{k,world}$ can be obtained by using the estimated vehicle position x_k which contains the vehicle's heading angle ψ_k, and the vehicle's global position X_k and Y_k. The rotation matrix $R_{k,world}$ consists of the trigonometrical function with the vehicle's heading angle ψ_k from the estimated vehicle position x_k. The translation matrix $T_{k,world}$ consists of the relative position from the vehicle's global position X_k and Y_k as described in (17).

$$R_{k,world} = \begin{bmatrix} \cos(\psi_k) & -\sin(\psi_k) \\ \sin(\psi_k) & \cos(\psi_k) \end{bmatrix}$$
$$T_{k,world} = \begin{bmatrix} X_k \\ Y_k \end{bmatrix} \quad (17)$$

The converted position of each node of the lane geometry map can be obtained by applying the translation matrix $T_{k,world}$ and rotation matrix $R_{k,world}$ as described in (18).

$$\begin{bmatrix} X_{i,j,world} \\ Y_{i,j,world} \end{bmatrix} = R_{k,world}\begin{bmatrix} X_{i,j,ego} \\ Y_{i,j,ego} \end{bmatrix} + T_{k,world} \quad (18)$$

VI. LANE GEOMETRY MODELING

Each lane in the lane geometry map generated from the previous probabilistic lane smoothing step is represented as a number of the nodes. Because the lane representation using a number of the nodes is not suitable for the application of the intelligent vehicles, the lane geometry map is modeled to the mathematical curve model in the lane geometry modeling step. In order to reduce the number of representations of the lane geometry map, the lane geometry map is modeled as a B-spline curve as proposed in [43].

A. B-SPLINE CURVE

The B-spline curve is one of the representations of the spline curve which consists of control points, knot vectors, and basis functions. Since each section is represented by a separate polynomial, the B-spline curve has a property that even if a part of the control points is changed, the entire curve is not affected. Additionally, comparing with the conventional lane geometry representation, the lane geometry representation with the B-spline curve has an advantage that it is simple to express mathematically. The B-spline curve $C(t)$ can be represented using the parametric spline equation as described in (19). p means the order of the spline. b_j is a set of the control points and t is a parameter of the spline.

$$C(t) = \sum_{j=0}^{n} N_{j,p}(t)b_j, \quad t \in [T_{p-1}, T_{n+1}] \quad (19)$$

The knot vector T which contains a non-decreasing sequence of real value is described in (20).

$$T = [T_0, T_1, \ldots, T_{n+p-1}, T_{n+p}] \quad (20)$$

In order to fix the endpoints of the spline curve to the endpoints of control points, the first and last set of knots are defined with the same value as described in (21).

S. Kim *et al.*: Probabilistic Smoothing Based Generation of a Reliable Lane Geometry Map With Uncertainty of a Lane Detector

IEEE *Access*

t_{start} and t_{end} means the parameter of the endpoints of the spline curve.

$$T_0 = T_1 = \cdots = T_{p-1} = t_{start}$$
$$T_{n+1} = T_{n+2} = \cdots = T_{n+p} = t_{end} \quad (21)$$

$N_{j,p}(t)$ is the basis function of the spline curve with order p as described in (22).

$$N_{i,0}(t) = \begin{cases} 1, & if \ t \in [T_i, T_{i+1}] \\ 0, & otherwise \end{cases}$$
$$N_{i,j}(t) = \frac{t - T_j}{T_{i+j} - T_i} N_{i,j-1}(t)$$
$$+ \frac{T_{i+j-1} - t}{T_{i+j-1} - T_{i+1}} N_{i+1,j-1}(t) \quad (22)$$

B. GRADUAL CORRECTION METHOD-BASED LANE GEOMETRY MODELING

The nodes of the lane geometry map from the probabilistic lane smoothing step are modeled as a B-spline curve using the gradual correction method. For modeling as the B-spline curve, the several factors of the B-spline curve such as the number of control points, the order of the spline, and knots vector should be determined. Among these factors, the number of control points is the dominant factor for modeling the lane geometry because it affects the quality and data storage of the lane geometry map. The gradual correction method which provides a suboptimal solution about the number of control points and other factors is used. The process of the lane geometry modeling consists of following two steps.

1) INITIALIZATION

The interval between the nodes is irregular because the new node is not generated with a regular interval and the position of each node is updated probabilistically. Therefore, the spatial resampling is performed by resampling the sequential points p_i with regular intervals.

The parameter of the resampled sequential points p_i is calculated based on the chord length parameterization method. The parameter t_i can be obtained from the chord length that is the distance between the two adjacent points as described in (23).

$$t_i = \sum_{j=0}^{i} \Delta_j, \quad where \ \Delta_j = |p_j - p_{j-1}| \quad (23)$$

When the B-spline model is approximated using the gradual correction method, the principal parameter vector should be constructed. The minimum number p of the principal parameters are required for the lane geometry model using the p-order B-spline. The initial principal parameter vector is constructed using uniformly divided values of the parameter

value t_i as described in (24).

$$T_{principal} = \begin{bmatrix} 0 \\ t_{round(\frac{1}{p-1}m)} \\ t_{round(\frac{2}{p-1}m)} \\ \cdots \\ t_m \end{bmatrix}^T \quad (24)$$

2) GRADUAL CORRECTION METHOD

In the gradual correction method, the error between the lane geometry map data and the B-spline model is gradually corrected until the error is less than an acceptable tolerance range. Based on the principal parameter vector, the knots can be determined. The knot vector T is constructed by using the average of the principal parameter vector $T_{principal}$ as described in (25). The τ_j are the elements of the principal parameter vector $T_{principal}$ containing $k + 1$ elements.

$$T_{p+i-1} = \frac{1}{p-1} \sum_{j=i}^{i+p-2} \tau_j, \quad i = 1, \ldots, k - p + 1 \quad (25)$$

Addition to the principal parameter vector $T_{principal}$ and knot vector T, the control points b_j is needed to approximate the B-spline model. The control points are determined applying the least square method for minimizing the error between the approximated B-spline curve and the resampled sequential points p_i as described in (26).

$$E(b_0, \ldots, b_n) = \sum_{i=0}^{m} \left\| C(\bar{t}_i) - p_i \right\|^2 \quad (26)$$

If the maximum error is larger than the acceptable tolerance range, the new principal parameter vector should be updated. The new element of the principal parameter vector is determined as a parameter of the dominant point for the resampled sequential points p_i. The dominant point can be determined by using the segment region error. The segment region error-based dominant point selection method can prevent the unstable problem caused by a concentration of the principal parameters and knots on the small curve region. The segment region error can be calculated by the trapezoidal method as described in (27). s means the start resampled sequential point and e is the end resampled sequential point in each segment. err_i means the error between the approximated B-spline curve and the resampled sequential points p_i. The dominant point is selected as the maximum error point in the region with the maximum segment region error.

$$err_{segment} = \sum_{i=s}^{e-1} \frac{(err_i + err_{i+1})(t_{i+1} - t_i)}{2} \quad (27)$$

By using the new principal parameter vector, the knot vector T and the control points b_j can be obtained based on (25) and (26). After obtaining the new principal parameter vector,

IEEE *Access*

S. Kim *et al.*: Probabilistic Smoothing Based Generation of a Reliable Lane Geometry Map With Uncertainty of a Lane Detector

TABLE 1. Vehicle motion sensor specification.

Sensor	Frequency	Range	Resolution	Noise (RMS)	Unit
Yaw rate	50 Hz	± 120	0.0625	0.5	deg/sec
Wheel speed	50 Hz	0 - 130	0.035	0.3	m/s

TABLE 2. Vehicle motion sensor specification.

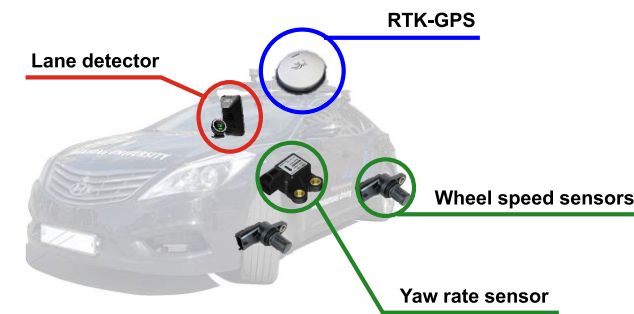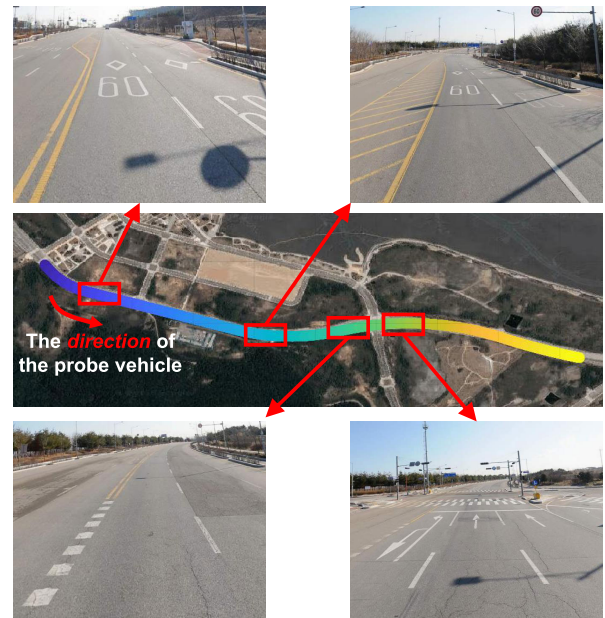| GPS receivers		RTK-GPS
Accuracy (RMS)	Position	2 cm
	Velocity	0.03 m/s
Data rate		Up to 50 Hz

FIGURE 10. Sensor configuration of the probe vehicle.

the knot vector, and the control points, the improved B-spline curve for lane geometry map is able to be approximated. If the maximum error between the improved B-spline curve and the resampled sequential points p_i is larger than the acceptable tolerance range, the gradual correction method is iteratively executed to make the maximum error under the acceptable tolerance error.

VII. EXPERIMENTAL RESULTS

A. EXPERIMENTAL ENVIRONMENTS

In order to evaluate the proposed method, the probe vehicle which equipped with a lane detector, RTK-GPS, vehicle motion sensors is used as shown in Fig. 10. When the probe vehicle drives, the raw data such as the detected lane information, vehicle motion information, and vehicle position information are acquired with time synchronization.

In order to obtain the vehicle motion information, the yaw rate sensor and wheel speed sensors are used. The specifications of the vehicle motion sensors are described in Table 2. Since the yaw rate can be filtered with a simple mathematical model, the yaw rate sensor is used for estimating the rotation motion. The vehicle motion information is obtained from the Controller Area Network (CAN) without installing additional sensors because the probe vehicle is equipped an Electronic Stability Control (ESC) system.

In this article, the probe vehicle's position is acquired from the RTK-GPS. The RTK-GPS has a centimeter-level accuracy about the position. The detail specifications of the RTK-GPS are described in Table 1. For detecting the lane

(a)

(b)

FIGURE 11. Test site (a) Aerial image and road images of the test site, (b) The precise lane marker map about the test site.

information, the Mobileye Q3 is used. The lane detector provides the lane information in the forms of a cubic polynomial on the coordinates of the ego vehicle. The length of the detected lane and the quality of the detected lane information which indicates the reliability are also provided. From this information, the detected lane information can be used selectively.

In order to evaluate the generated lane geometry map from the proposed method, the test site is selected where the precise lane marker map was already constructed. The road of test site contains the shadow of the traffic signs, different types of lane, and cracks which can increase inaccuracy of the lane detector as shown in Fig. 11-(a). Because the lane can be blocked by surrounding vehicles consistently, the probe vehicle accumulates the lane information with low traffic condition, so that the lane detector could detect lanes. The travel distance of the selected test site is about 1.6 *km*. The precise lane marker map for the evaluation was
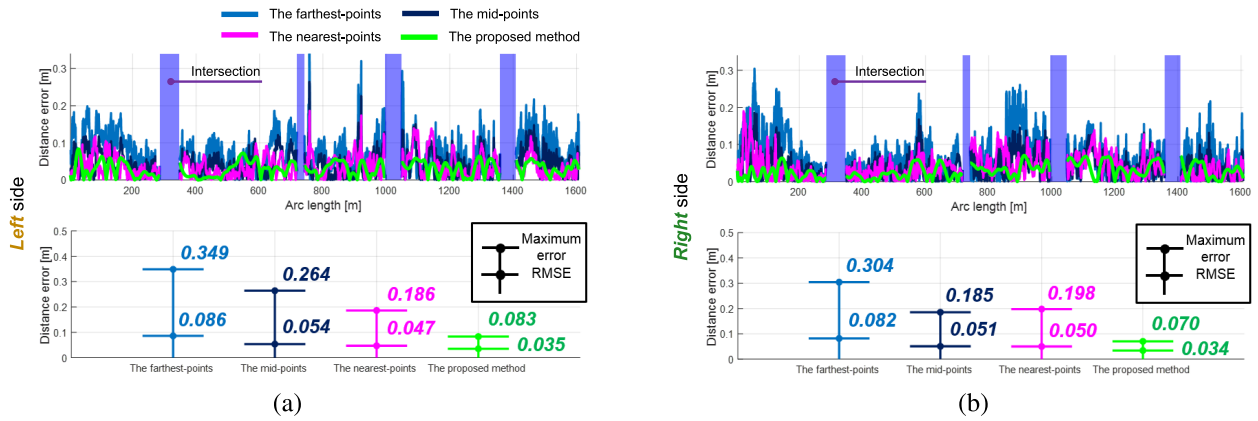
S. Kim *et al.*: Probabilistic Smoothing Based Generation of a Reliable Lane Geometry Map With Uncertainty of a Lane Detector

IEEE *Access*

FIGURE 12. Evaluation results of the distance error (a) Left lane geometry map, (b) Right lane geometry map.
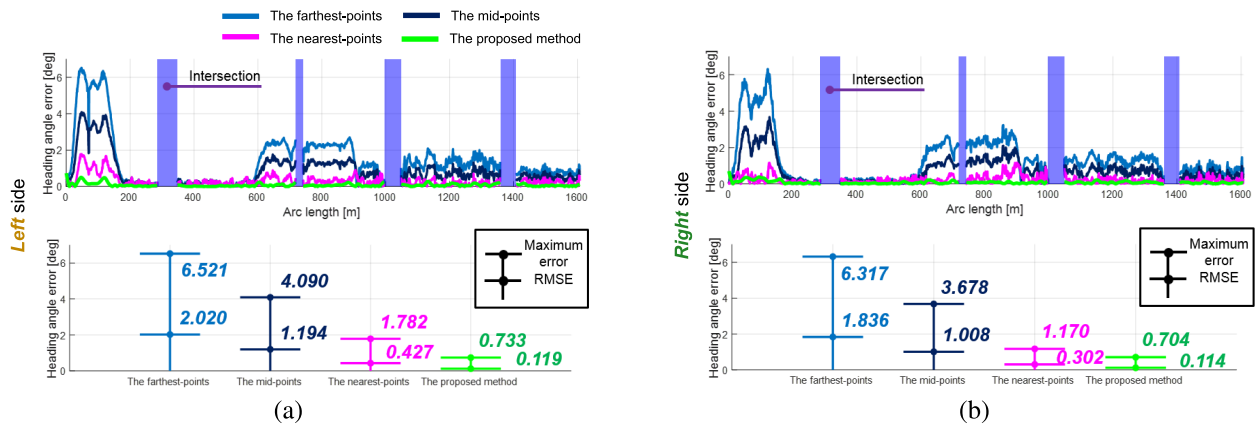

FIGURE 13. Evaluation results of the heading angle error (a) Left lane geometry map, (b) Right lane geometry map.

precisely generated manually to remove the fault features and add the undetected road surface marker feature as shown in Fig. 11-(b) [46]. The 3431 time-synchronized data about the detected lane information, vehicle motion information, and vehicle position information are acquired when the probe vehicle was driving in this test site and are used to generate the lane geometry map.
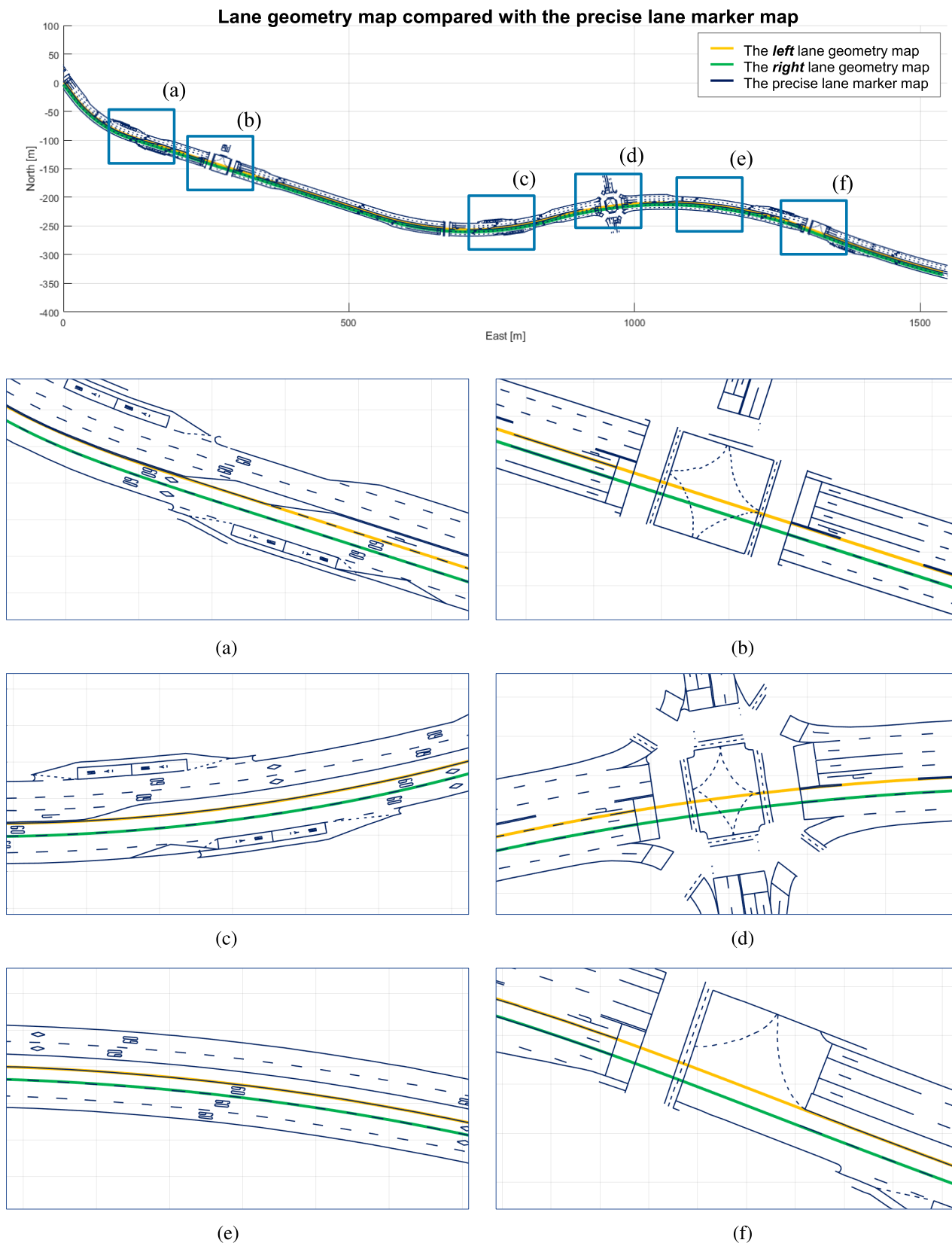
B. COMPARISON WITH THE PRECISE LANE MARKER MAP

As mentioned in the previous section, the generated lane geometry map is evaluated by comparing the precise lane marker map. In order to indicate the location of the lane geometry map, the location of the lane geometry map is separated by the left side and the right side based on the direction of the probe vehicle. The generated lane geometry map with the precise lane marker map is described in Fig. 14. The lane geometry curves of the left and right lane geometry map are fitted qualitatively with the precise lane marker map in case of the solid and dashed lane marker as shown in Fig. 14-(a), (c), (e). Additionally, in lane geometry modeling step of the proposed method, the lane geometry map was modeled as the mathematical curve using the nodes of each

lane. Therefore, the lane geometry map can be generated by interpolating the no lane conditions such as intersection as shown

in Fig. 14-(b), (d), (f). In the follows in this section, the generated lane geometry is evaluated on the distance error and the heading angle error to check how it fits well with the ground truth and how the noise of the detected lane information is reduced.

1) DISTANCE ERROR

In order to check how the noise of the detected lane information is reduced and how the generated lane geometry map fits well, the lane geometry maps which are generated by using the sampled points are also evaluated. Since the reliability of the detected lane information depends on the distance from the lane detector, the sampled points are selected based on the distance from the sensor. The results of the distance error between the ground truth, and the generated lane geometry map from the sampled points and the proposed method are described in Fig. 12. In the intersection area, the distance error cannot be calculated because the ground truth does not exist. Therefore, the maximum distance error

IEEE *Access*

S. Kim *et al.*: Probabilistic Smoothing Based Generation of a Reliable Lane Geometry Map With Uncertainty of a Lane Detector

Lane geometry map compared with the precise lane marker map

FIGURE 14. The generated lane geometry map compared with the precise lane marker map (a), (c), (e) The lane geometry map on the solid and dashed lane marker, (b), (d), (f) The lane geometry map on the intersection.

S. Kim *et al.*: Probabilistic Smoothing Based Generation of a Reliable Lane Geometry Map With Uncertainty of a Lane Detector

IEEE *Access*

and Root Mean Square Error (RMSE) are only obtained in the non-intersection area.

In the case of the left lane geometry map, the maximum distance error of each lane geometry map generated from the farthest-, the mid-, and the nearest-points of the detected lane information is 0.349 *m*, 0.264 *m*, and 0.186 *m*. By applying the proposed method to generate the lane geometry map, the maximum distance error can be reduced to 0.083 *m*. The RMSE is also reduced from 0.047 *m* to 0.035 *m* comparing with the lane geometry map generated from the nearest-points as shown in Fig. 12-(a).

Similar to the left lane geometry map, the maximum distance error of the right lane geometry map is reduced from 0.304 *m*, 0.185 *m*, and 0.198 *m* to 0.070 *m* comparing with the lane geometry map generated from the farthest-, mid-, nearest-points. The RMSE is also reduced from 0.050 *m* to 0.034 *m* comparing with the lane geometry map generated from the nearest-points as shown in Fig. 12-(b). Since the width of the lane marker is about 0.15 0.20 *m*, the maximum distance error and the RMSE of the left and right lane geometry map generated from the proposed method are acceptable.

2) HEADING ANGLE ERROR

In the same as the distance error comparison, the lane geometry maps which are generated by using the sampled points are also evaluated to check how the noise of the detected lane information is reduced. The results of the heading angle error between the ground truth, and the generated lane geometry map from the sampled points and the proposed method are described in Fig. 13. In the intersection area, the heading angle error cannot be calculated because the ground truth does not exist. Therefore, the maximum heading angle error and RMSE are only obtained in the non-intersection area.

In the case of the left lane geometry map, the maximum heading angle error of each lane geometry map generated from the farthest-, the mid-, and the nearest-points of the detected lane information is 6.521 *deg*, 4.090 *deg*, and 1.782 *deg*. By applying the proposed method to generate the lane geometry map, the maximum heading angle error can be reduced to 0.733 *deg*. The RMSE is also reduced from 0.427 *deg* to 0.119 *deg* comparing with the lane geometry map generated from the nearest-points as shown in Fig. 13-(a).

Similar to the left lane geometry map, the maximum heading angle error of the right lane geometry map is reduced from 6.317 *deg*, 3.678 *deg*, and 1.170 *deg* to 0.704 *deg* comparing with the lane geometry map generated from the farthest-, mid-, nearest-points. The RMSE is also reduced from 0.302 *deg* to 0.114 *deg* comparing with the lane geometry map generated from the nearest-points as shown in Fig. 13-(b). When the intelligent vehicle uses the lane geometry information 100 *m* ahead to the longitudinal direction, the RMSE (0.119 *deg* and 0.114 *deg*) of each lane geometry map generated from the proposed method causes 0.208 *m* and 0.119 *m* lateral errors. Since the width of the lane marker is about 0.15 0.20 *m*, the heading angle error of each lane geometry map is acceptable.

VIII. CONCLUSION

This article has presented a probabilistic smoothing-based generation method of the reliable lane geometry map. In order to use the lane geometry map for the lane geometry information in the intelligent vehicle, the lane geometry map should guarantee its accuracy. Since the lane curve accumulated by the probe vehicle contains the noise caused by the resolution of the sensor and vehicle motion, the acquired data is refined through the probabilistic smoothing technique to reduce the effect of the sensor noise. In the probabilistic smoothing technique, the lane geometry map is modeled as the nodes with the uncertainty of each node's position obtained from sensor error model. The position and uncertainty of each node are updated by the Bayesian filtering scheme. The proposed map generation method also contains the process of vehicle trajectory estimation and lane geometry modeling. In the vehicle trajectory estimation step, the reliability of RTK-GPS can be improved by the RTS smoothing with the RTK-GPS and vehicle motion information. The generated lane geometry map is modeled as a B-spline curve model by using the gradual correction method for reducing the data storage of the lane geometry map in lane geometry modeling step. The experimental results showed that the noise of the detected lane curve could be reduced by using the probabilistic lane smoothing algorithm and the generated lane geometry has a reliable accuracy for using the intelligent vehicle in terms of distance error and heading angle error.

Although the proposed method can be used to generate the reliable lane geometry map, the various road conditions were not considered; for example, road connection relationship in an intersection, and lane split and merge condition. Therefore, the author plans to improve the proposed algorithm for covering the upper various road conditions.

REFERENCES

[1] NHTSA. (2019). *Automated Vehicles for Safety*. [Online]. Available: https://www.nhtsa.gov/technology-innovation/automated-vehicles-safety

[2] O. Gusikhin, D. Filev, and N. Rychtyckyj, "Intelligent vehicle systems: Applications and new trends," in *Informatics in Control Automation and Robotics*. Springer, 2008, pp. 3–14.

[3] R. Bishop, *Intelligent Vehicle Technology and Trends*. 2005.

[4] S. Tsugawa, "Vision-based vehicles in Japan: Machine vision systems and driving control systems," *IEEE Trans. Ind. Electron.*, vol. 41, no. 4, pp. 398–405, Aug. 1994.

[5] P. Falcone, F. Borrelli, J. Asgari, H. E. Tseng, and D. Hrovat, "Predictive active steering control for autonomous vehicle systems," *IEEE Trans. Control Syst. Technol.*, vol. 15, no. 3, pp. 566–580, May 2007.

[6] S.-W. Kim, W. Liu, M. H. Ang, E. Frazzoli, and D. Rus, "The impact of cooperative perception on decision making and planning of autonomous vehicles," *IEEE Intell. Transp. Syst. Mag.*, vol. 7, no. 3, pp. 39–50, Jul. 2015.

[7] C. Urmson *et al.*, "Autonomous driving in urban environments: Boss and the urban challenge," *J. Field Robot.*, vol. 25, no. 8, pp. 425–466, 2008.

[8] K. Chu, M. Lee, and M. Sunwoo, "Local path planning for off-road autonomous driving with avoidance of static obstacles," *IEEE Trans. Intell. Transp. Syst.*, vol. 13, no. 4, pp. 1599–1616, Dec. 2012.

[9] J. E. Naranjo, C. Gonzalez, R. Garcia, and T. de Pedro, "Lane-change fuzzy control in autonomous vehicles for the overtaking maneuver," *IEEE Trans. Intell. Transp. Syst.*, vol. 9, no. 3, pp. 438–450, Sep. 2008.

[10] R. Toledo-Moreo, D. Betaille, F. Peyret, and J. Laneurit, "Fusing GNSS, dead-reckoning, and enhanced maps for road vehicle lane-level navigation," *IEEE J. Sel. Topics Signal Process.*, vol. 3, no. 5, pp. 798–809, Oct. 2009.

IEEE Access

S. Kim *et al.*: Probabilistic Smoothing Based Generation of a Reliable Lane Geometry Map With Uncertainty of a Lane Detector

[11] R. Toledo-Moreo, D. Betaille, and F. Peyret, "Lane-level integrity provision for navigation and map matching with GNSS, dead reckoning, and enhanced maps," *IEEE Trans. Intell. Transp. Syst.*, vol. 11, no. 1, pp. 100–112, Mar. 2010.

[12] Z. Tao, P. Bonnifait, V. Fremont, and J. Ibanez-Guzman, "Mapping and localization using GPS, lane markings and proprioceptive sensors," in *Proc. IEEE/RSJ Int. Conf. Intell. Robots Syst.*, Nov. 2013, pp. 406–412.

[13] N. Suganuma and T. Uozumi, "Precise position estimation of autonomous vehicle based on map-matching," in *Proc. IEEE Intell. Vehicles Symp. (IV)*, Jun. 2011, pp. 296–301.

[14] M. Schreiber, C. Knoppel, and U. Franke, "LaneLoc: Lane marking based localization using highly accurate maps," in *Proc. IEEE Intell. Vehicles Symp. (IV)*, Jun. 2013, pp. 449–454.

[15] A. Schindler, "Vehicle self-localization with high-precision digital maps," in *Proc. IEEE Intell. Vehicles Symp. Workshops (IV Workshops)*, Jun. 2013, pp. 134–139.

[16] C. Lee and J.-H. Moon, "Robust lane detection and tracking for real-time applications," *IEEE Trans. Intell. Transp. Syst.*, vol. 19, no. 12, pp. 4043–4048, Dec. 2018.

[17] D.-K. Lee, J.-S. Shin, J.-H. Jung, S.-J. Park, S.-J. Oh, and I.-S. Lee, "Real-time lane detection and tracking system using simple filter and Kalman filter," in *Proc. 9th Int. Conf. Ubiquitous Future Netw. (ICUFN)*, Jul. 2017, pp. 275–277.

[18] K. H. Lim, K. P. Seng, L.-M. Ang, and S. W. Chin, "Lane detection and Kalman-based linear-parabolic lane tracking," in *Proc. Int. Conf. Intell. Hum.-Mach. Syst. Cybern.*, 2009, pp. 351–354.

[19] Z. Kim, "Robust lane detection and tracking in challenging scenarios," *IEEE Trans. Intell. Transp. Syst.*, vol. 9, no. 1, pp. 16–26, Mar. 2008.

[20] A. Borkar, M. Hayes, and M. T. Smith, "Robust lane detection and tracking with ransac and Kalman filter," in *Proc. 16th IEEE Int. Conf. Image Process. (ICIP)*, Nov. 2009, pp. 3261–3264.

[21] H. Weigel, H. Cramer, G. Wanielik, A. Polychronopoulos, and A. Saroldi, "Accurate road geometry estimation for a safe speed application," in *Proc. IEEE Intell. Vehicles Symp.*, Jun. 2006, pp. 516–521.

[22] P. Bender, J. Ziegler, and C. Stiller, "Lanelets: Efficient map representation for autonomous driving," in *Proc. IEEE Intell. Vehicles Symp.*, Jun. 2014, pp. 420–425.

[23] M. Tsogas, N. Floudas, P. Lytrivis, A. Amditis, and A. Polychronopoulos, "Combined lane and road attributes extraction by fusing data from digital map, laser scanner and camera," *Inf. Fusion*, vol. 12, no. 1, pp. 28–36, Jan. 2011.

[24] A. Chen, A. Ramanandan, and J. A. Farrell, "High-precision lane-level road map building for vehicle navigation," in *Proc. IEEE/ION Position, Location Navigat. Symp.*, May 2010, pp. 1035–1042.

[25] G.-P. Gwon, W.-S. Hur, S.-W. Kim, and S.-W. Seo, "Generation of a precise and efficient lane-level road map for intelligent vehicle systems," *IEEE Trans. Veh. Technol.*, vol. 66, no. 6, pp. 4517–4533, Jun. 2017.

[26] R. Rajamani, *Vehicle Dynamics and Control*. Springer, 2011.

[27] R. P. D. Vivacqua, M. Bertozzi, P. Cerri, F. N. Martins, and R. F. Vassallo, "Self-localization based on visual lane marking maps: An accurate low-cost approach for autonomous driving," *IEEE Trans. Intell. Transp. Syst.*, vol. 19, no. 2, pp. 582–597, Feb. 2018.

[28] D. Kim, T. Chung, and K. Yi, "Lane map building and localization for automated driving using 2D laser rangefinder," in *Proc. IEEE Intell. Vehicles Symp. (IV)*, Jun. 2015, pp. 680–685.

[29] O. Pink and C. Stiller, "Automated map generation from aerial images for precise vehicle localization," in *Proc. 13th Int. IEEE Conf. Intell. Transp. Syst.*, Sep. 2010, pp. 1517–1522.

[30] Y.-W. Seo, C. Urmson, and D. Wettergreen, "Exploiting publicly available cartographic resources for aerial image analysis," in *Proc. 20th Int. Conf. Adv. Geographic Inf. Syst. (SIGSPATIAL)*, 2012, pp. 109–118.

[31] M. Amo, F. Martínez, and M. Torre, "Road extraction from aerial images using a region competition algorithm," *IEEE Trans. Image Process.*, vol. 15, no. 5, pp. 1192–1201, Apr. 2006.

[32] J. Hu, A. Razdan, J. C. Femiani, M. Cui, and P. Wonka, "Road network extraction and intersection detection from aerial images by tracking road footprints," *IEEE Trans. Geosci. Remote Sens.*, vol. 45, no. 12, pp. 4144–4157, Dec. 2007.

[33] A. Joshi and M. R. James, "Generation of accurate lane-level maps from coarse prior maps and lidar," *IEEE Intell. Transp. Syst. Mag.*, vol. 7, no. 1, pp. 19–29, 2015.

[34] C. Guo, K. Kidono, J. Meguro, Y. Kojima, M. Ogawa, and T. Naito, "A low-cost solution for automatic lane-level map generation using conventional in-car sensors," *IEEE Trans. Intell. Transp. Syst.*, vol. 17, no. 8, pp. 2355–2366, Aug. 2016.

[35] A. Schindler, G. Maier, and F. Janda, "Generation of high precision digital maps using circular arc splines," in *Proc. IEEE Intell. Vehicles Symp.*, Jun. 2012, pp. 246–251.

[36] J. Ziegler *et al.*, "Making bertha drive—An autonomous journey on a historic route," *IEEE Intell. Transp. Syst. Mag.*, vol. 6, no. 2, pp. 8–20, 2014.

[37] X. Chen, B. Kohlmeyer, M. Stroila, N. Alwar, R. Wang, and J. Bach, "Next generation map making: Geo-referenced ground-level LIDAR point clouds for automatic retro-reflective road feature extraction," in *Proc. 17th ACM SIGSPATIAL Int. Conf. Adv. Geogr. Inf. Syst. (GIS)*, 2009, pp. 488–491.

[38] A. Boyko and T. Funkhouser, "Extracting roads from dense point clouds in large scale urban environment," *ISPRS J. Photogramm. Remote Sens.*, vol. 66, no. 6, pp. S2–S12, Dec. 2011.

[39] A. Mancini, E. Frontoni, and P. Zingaretti, "Automatic road object extraction from mobile mapping systems," in *Proc. IEEE/ASME 8th IEEE/ASME Int. Conf. Mech. Embedded Syst. Appl.*, Jul. 2012, pp. 281–286.

[40] H. Guan, J. Li, Y. Yu, C. Wang, M. Chapman, and B. Yang, "Using mobile laser scanning data for automated extraction of road markings," *ISPRS J. Photogramm. Remote Sens.*, vol. 87, pp. 93–107, Jan. 2014.

[41] D. Betaille and R. Toledo-Moreo, "Creating enhanced maps for lane-level vehicle navigation," *IEEE Trans. Intell. Transp. Syst.*, vol. 11, no. 4, pp. 786–798, Dec. 2010.

[42] D. Betaille, R. Toledo-Moreo, and J. Laneurit, "Making an enhanced map for lane location based services," in *Proc. 11th Int. IEEE Conf. Intell. Transp. Syst.*, Oct. 2008, pp. 711–716.

[43] K. Jo and M. Sunwoo, "Generation of a precise roadway map for autonomous cars," *IEEE Trans. Intell. Transp. Syst.*, vol. 15, no. 3, pp. 925–937, Jun. 2014.

[44] D. Simon, *Optimal State Estimation: Kalman, H Infinity, and Nonlinear Approaches*. Hoboken, NJ, USA: Wiley, 2006.

[45] S. Thrun, W. Burgard, and D. Fox, *Probabilistic Robotics*. Cambridge, MA, USA: MIT Press, 2005.

[46] K. Jo, Y. Jo, J. K. Suhr, H. G. Jung, and M. Sunwoo, "Precise localization of an autonomous car based on probabilistic noise models of road surface marker features using multiple cameras," *IEEE Trans. Intell. Transp. Syst.*, vol. 16, no. 6, pp. 3377–3392, Dec. 2015.

SEOKWON KIM (Student Member, IEEE) received the B.S. and M.S. degrees in automotive engineering from Hanyang University, Seoul, South Korea, in 2017 and 2019, respectively.

In M.S. course, he studied about autonomous driving systems, embedded system for autonomous, information fusion theories, and perception with the Automotive Control and Electronics Laboratory (ACE Lab). He currently works as a System Engineer with Mando Corporation for designing advanced driving assistance systems, such as lane centering steering, lane change assist, highway driving assist, and navigation-based adaptive cruise control.

MINCHUL LEE (Member, IEEE) received the B.S. degree in mechanical engineering from Hanyang University, Seoul, South Korea, in 2013, where he is currently pursuing the Ph.D. degree with the Automotive Control and Electronics Laboratory (ACE Lab). His main research interests include driving environment assessment, precise positioning and localization, information fusion theories, and real-time systems for autonomous. His current research interest includes vehicle motion assessment for an autonomous car.

S. Kim *et al.*: Probabilistic Smoothing Based Generation of a Reliable Lane Geometry Map With Uncertainty of a Lane Detector

IEEE *Access*

MYOUNGHO SUNWOO (Life Member, IEEE) received the B.S. degree in electrical engineering from Hanyang University, in 1979, the M.S. degree in electrical engineering from The University of Texas at Austin, in 1983, and the Ph.D. degree in system engineering from Oakland University, in 1990. He joined General Motors Research (GMR) Laboratories, Warren, MI, in 1985, where he has worked in the area of automotive electronics and control for 30 years. During his nine-year tenure at GMR, he has worked on the design and development of various electronic control systems for powertrains and chassis. Since 1993, he has led research activities as a Professor with the Department of Automotive Engineering, Hanyang University. His work has focused on automotive electronics and controls (such as modeling and control of internal combustion engines, design of automotive distributed real-time control systems, intelligent autonomous vehicles, and automotive education programs).

KICHUN JO (Member, IEEE) received the B.S. degree in mechanical engineering and the Ph.D. degree in automotive engineering from Hanyang University, Seoul, South Korea, in 2008 and 2014, respectively. From 2014 to 2015, he was with the ACE Laboratory, Department of Automotive Engineering, Hanyang University, doing research on system design and implementation of autonomous cars. From 2015 to 2018, he was with the Valeo Driving Assistance Research, Bobigny, France, working on the highly automated driving. He is currently an Assistant Professor with the Department of Smart Vehicle Engineering, Konkuk University, Seoul. His current research interests include localization and mapping, objects tracking, information fusion, vehicle state estimation, behavior planning, and vehicle motion control for highly automated vehicles.

● ● ●